

Possible gapless spin liquid in a rare-earth kagomé lattice magnets $\text{Tm}_3\text{Sb}_3\text{Zn}_2\text{O}_{14}$

Zhao-Feng Ding¹, Yan-Xing Yang¹, Jian Zhang¹, Cheng Tan¹, Zi-Hao Zhu¹, Gang Chen^{1,2,3,*} and Lei Shu^{1,3†}

¹State Key Laboratory of Surface Physics, Department of Physics, Fudan University, Shanghai 200433, China

²Center for Field Theory and Particle Physics, Fudan University, Shanghai 200433, China and

³Collaborative Innovation Center of Advanced Microstructures, Nanjing University, Nanjing 210093, China

(Dated: February 19, 2022)

We report the thermodynamic and muon spin relaxation (μSR) evidences for a possible gapless spin liquid in $\text{Tm}_3\text{Sb}_3\text{Zn}_2\text{O}_{14}$, with the rare-earth ions Tm^{3+} forming a two-dimensional kagomé lattice. We extract the magnetic specific heat of $\text{Tm}_3\text{Sb}_3\text{Zn}_2\text{O}_{14}$ by subtracting the phonon contribution of the non-magnetic isostructural material $\text{La}_3\text{Sb}_3\text{Zn}_2\text{O}_{14}$ and obtain a clear linear- T temperature dependence of magnetic specific heat at low temperatures. No long-range magnetic order was observed down to 0.35 K in the heat capacity measurements, and no signature of spin freezing down to 50 mK was observed in A.C. susceptibility measurements. The absence of magnetic order is further confirmed by the μSR measurements down to 20 mK. We find that the spin-lattice relaxation time remains constant down to the lowest temperature. We point out that the physics in $\text{Tm}_3\text{Sb}_3\text{Zn}_2\text{O}_{14}$ is fundamentally different from the Cu-based herbertsmithite and propose spin liquid ground states with non-Kramers doublets on the kagomé lattice to account for the experimental results. However, we can not rule out that these exotic properties are induced by the Tm/Zn site-mixing disorder in $\text{Tm}_3\text{Sb}_3\text{Zn}_2\text{O}_{14}$.

I. INTRODUCTION

Quantum spin liquid (QSL) is an exotic quantum state of matter in which the spins are highly entangled and remain disordered even down to zero temperature. The search of QSLs has attracted a significant attention partly due to its potential application on quantum information and the possible relevance to high superconductivity^{1–4}. As a new quantum phase of matter beyond the traditional Landau's symmetry breaking paradigm, QSL has its own value. Instead of associating with certain order parameters for conventional symmetry breaking states, QSL is often characterized by the excitations with fractionalized spin quantum number and the emergent gauge structure. Precisely due to the absence of magnetic order, the experimental identification of QSLs requires more scrutiny than conventional orders. In the last decade or so, an increasing number of new materials have been proposed to be QSL candidates. These spin liquid candidates often have the lattice structures with geometric frustration such as triangle lattice (κ -[ET]₂Cu₂(CN)₃^{5–11}, EtMe₃Sb[Pd(dmit)₂]₂^{12–15}, and YbMgGaO₄^{16–33}), kagomé lattice (ZnCu₃(OH)₆Cl₂^{34–36}), hyperkagomé lattice (Na₄Ir₃O₈^{37–42}), and pyrochlore lattice (Yb₂Ti₂O₇^{43,44}, Pr₂Zr₂O₇⁴⁵, Pr₂Ir₂O₇^{46–52}, Tb₂Ti₂O₇^{53,54}, et al.), and our work here is about a rare-earth kagomé lattice magnet.

Recently, a new family of pyrochlore derivatives $RE_3\text{Sb}_3M_2\text{O}_{14}$ ($RE = \text{La, Pr, Nd, Gd, Tb, Dy, Ho, Er,}$ and Yb ; $M = \text{Mg, Zn}$) with a kagomé lattice structure was discovered, and their crystal structure, thermal transport, and magnetic properties were studied^{55–60}. In these materials, the rare-earth ions form two-dimensional kagomé lattice layers that are separated by non-magnetic Zn/Mg layer. Several magnetic phases including the emergent kagomé Ising order⁵⁸, non-magnetic singlet

state⁵⁹, spin glass⁵⁹, and even spin liquid⁵⁹ were proposed.

Despite the previous effort, one compound in this material family has not been carefully explored. Here, we study the magnetic properties of the compounds $\text{Tm}_3\text{Sb}_3\text{Zn}_2\text{O}_{14}$ in this family as well as a non-magnetic reference compound $\text{La}_3\text{Sb}_3\text{Zn}_2\text{O}_{14}$. The heat capacity measurements did not find any evidence of magnetic order for $\text{Tm}_3\text{Sb}_3\text{Zn}_2\text{O}_{14}$ down to ~ 0.35 K despite an antiferromagnetic Curie-Weiss temperature $\Theta_{\text{CW}} = -18.6$ K. A linear- T heat capacity is obtained at low temperatures, indicating a constant density of states and gapless excitations at low energies. No spin freezing was observed in A.C. magnetic susceptibility measurements. The absence of the magnetic order is further confirmed by the muon spin relaxation (μSR) measurements. The constant spin lattice relaxation rate at low energies seems to be consistent with the large and constant density of states at low energies in this system. We discuss the microscopic origin of the Tm^{3+} local moments, propose the candidate spin liquid ground states with either spinon Fermi surface or spinon quadratic node and further experiments for $\text{Tm}_3\text{Sb}_3\text{Zn}_2\text{O}_{14}$. Inspired by a recent theoretical study of the effect of quenched bond disorder on spin-1/2 quantum magnets⁶¹, the possibility of Tm/Zn site-mixing disorder induced localized two-level scenario can not be excluded.

II. EXPERIMENTAL DETAILS

The polycrystalline $RE_3\text{Sb}_3\text{Zn}_2\text{O}_{14}$ ($RE = \text{La, Tm}$) samples were synthesized by solid state reaction method as reported before⁵⁵. The sample structure was confirmed by powder X-ray diffraction (XRD) measurements (Bruker D8 Advance, $\lambda = 1.5418$ Å) at room temperature. Rietveld crystal structure refinements of

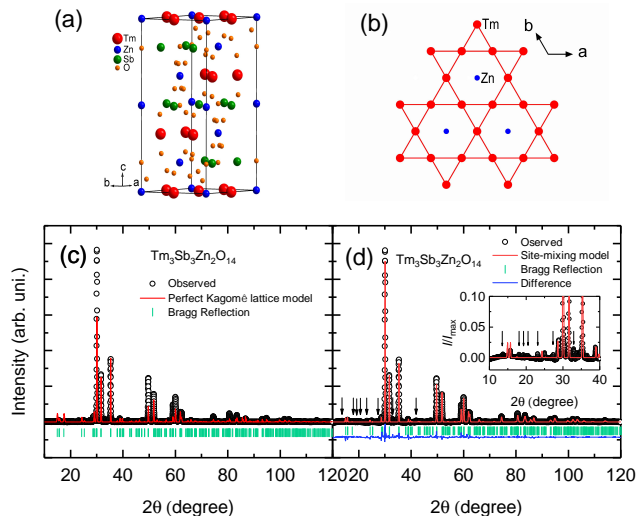


FIG. 1. (a) Crystal structure of $\text{Tm}_3\text{Sb}_3\text{Zn}_2\text{O}_{14}$ in one unit cell. (b) The kagomé lattice formed by the Tm^{3+} ions in the ab plane. The position of in-plane Zn^{2+} was also shown. (c) Rietveld refinement of powder XRD pattern for $\text{Tm}_3\text{Sb}_3\text{Zn}_2\text{O}_{14}$ using the perfect kagomé lattice model, which cannot describe the data well. The green bars indicate the Bragg reflections. (d) Rietveld refinement of powder XRD pattern for $\text{Tm}_3\text{Sb}_3\text{Zn}_2\text{O}_{14}$ using site-mixing model. The black circles, red line, and blue line are the experimental data, the calculated patterns based on the Tm/Zn site-mixing model and the differences, respectively. The green bars indicate the Bragg reflections. Inset is the enlargement of the low degree part. The arrows indicate the tiny peaks that cannot be described by Tm/Zn site-mixing model.

the XRD data were performed by using GSAS program⁶² and EXPGUI⁶³.

Magnetization was measured in a superconducting quantum interference device magnetometer (Quantum Design Magnetic Property Measurement System) down to 2 K. A.C. susceptibility was measured in a Quantum Design Physical Property Measurement System (PPMS) equipped with A.C. Measurement System for the Dilution Refrigerator option in a temperature range of 0.05 - 4 K. Specific heat down to 0.35 K was measured by the adiabatic relaxation method on a Dynacool-PPMS platform equipped with Helium-3 option.

Zero field muon spin relaxation (ZF- μSR) experiments down to 20 mK were carried out by using the continuous beam line on the DR spectrometer at TRIUMF, Vancouver, Canada. During the μSR experiment, the powder sample was mounted on a silver sample holder using GE-varnish. Before the experiments, a weak transverse field run was carried out at 6 K to determine the value of α , which is the detector efficiency related to the experimental setup. ZF- μSR experiments were then carried out after zeroing the magnetic field by measuring the standard silver sample with method as introduced before⁶⁴.

III. RESULTS

A. Crystal Structure

Our sample quality was examined by the XRD and magnetic susceptibility measurements. The crystal structure of $\text{Tm}_3\text{Sb}_3\text{Zn}_2\text{O}_{14}$ is shown in Fig. 1(a). Fig. 1(b) shows the kagomé layer formed by Tm^{3+} ions. The typical XRD spectrum of $\text{Tm}_3\text{Sb}_3\text{Zn}_2\text{O}_{14}$ is depicted in Fig. 1(c) and (d). From Fig. 1(c), we notice that the low degree peaks below 30 degree of $\text{Tm}_3\text{Sb}_3\text{Zn}_2\text{O}_{14}$ are absent. This is inconsistent with the perfect kagomé lattice model. Similar behavior was also observed in $\text{RE}_3\text{Sb}_3\text{Zn}_2\text{O}_{14}$ (RE is rare earth element with ion radius smaller than Dy) and was explained by the RE/Zn site-mixing disorder in recent works^{59,60}. The XRD pattern of $\text{Tm}_3\text{Sb}_3\text{Zn}_2\text{O}_{14}$ is fitted by using the site-mixing model. Table I lists the fitting parameters using both perfect kagomé lattice model without disorder (fitted curve in Fig. 1(c)) and site-mixing model (fitted curve in Fig. 1(d)). It can be seen that the site-mixing model describes the data better, and it suggests that only $\sim 82.7\%$ of the Tm ions stay on their original position and $\sim 82.5\%$ Zn ions occupy the in-plane Zn sites. There are site-mixing between Tm and in-plane Zn ions. As shown in the main graph of Fig. 1(d), the site-mixing model can describe the main feature of the XRD pattern, despite of several additional tiny peaks indicated by arrows in inset of Fig. 1(d). Similar results were also observed in previous work, and it was suggested that the XRD pattern may be more accurately described by a different model⁵⁹. Since better model has not been found, we take the site-mixing of Tm/Zn as the main source of disorder in $\text{Tm}_3\text{Sb}_3\text{Zn}_2\text{O}_{14}$. The possible disorder effect will be discussed in the discussion section.

The distorted Tm kagomé layers are separated by the non-magnetic Zn, Sb and O atoms. The interlayer separation of the Tm kagomé layers is 5.67 Å. Since the Tm layers are not stacked right on top of each other, the nearest Tm-Tm bond between two neighboring layers is actually larger than the interlayer separation and is 6.06 Å. Within the kagomé layers, the nearest Tm-Tm bond is 3.68 Å and is much smaller than the interlayer Tm-Tm bonds. This justifies the quasi-two-dimensional nature of $\text{Tm}_3\text{Sb}_3\text{Zn}_2\text{O}_{14}$.

B. Magnetization

The magnetic susceptibility of $\text{Tm}_3\text{Sb}_3\text{Zn}_2\text{O}_{14}$ was measured under an external field of $\mu_0 H = 0.01$ T down to 2 K and is depicted in Fig. 2(a). As shown in Fig. 2(b), the Curie-Weiss law behaviour is observed in high temperature range. The Curie-Weiss law fitting in the range of 10 - 20 K (the most Curie-Weiss like region, just above the Schottky anomaly observed in specific heat) yields a Curie-Weiss temperature $\Theta_{\text{CW}} = -18.6$ K and an effective magnetic moment $\mu_{\text{eff}} = 7.50 \mu_B$. The

TABLE I. Rietveld fitting results using both perfect kagomé lattice model and site-mixing model.

Atom	Site	x	y	z	Occ.	a, b (Å)	c (Å)	χ^2
Perfect kagomé lattice model								
Tm	9	0.5	0	0	1	7.3446(2)	16.9930(6)	1547
Zn1	3	0	0	0	1			
Zn2	18	0	0	0.5	1			
Sb	9	0.5	0	0.5	1			
O1	6	0	0	0.326(6)	1			
O2	18	0.616(4)	-0.616(4)	0.227(3)	1			
O3	18	0.196(5)	-0.196(5)	-0.038(4)	1			
Site-mixing model								
Tm	9	0.5	0	0	0.827(6)	7.3568(2)	17.0196(7)	380
Zn(disorder)	9	0.5	0	0	0.173(6)			
Zn1	3	0	0	0	0.825(6)			
Tm(disorder)	3	0	0	0	0.175(6)			
Zn2	18	0	0	0.5	1			
Sb	9	0.5	0	0.5	1			
O1	6	0	0	0.326(3)	1			
O2	18	0.616(2)	-0.616(2)	0.234(1)	1			
O3	18	0.147(2)	-0.147(2)	-0.052(1)	1			

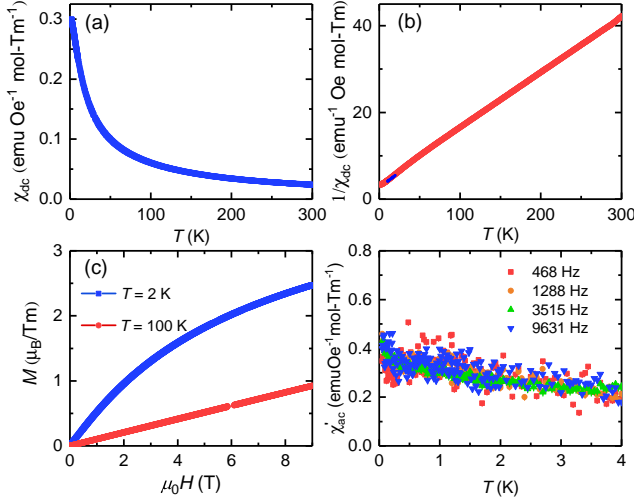


FIG. 2. Temperature dependence of magnetic susceptibility (a) and its inverse (b) of $\text{Tm}_3\text{Sb}_3\text{Zn}_2\text{O}_{14}$ under an applied magnetic field of $\mu_0 H = 0.01$ T. Blue line in (b) is the Curie-Weiss law fitting curve of the data between 10 and 20 K. (c) Isothermal magnetization up to 9 T at 2 K (blue squares) and 100 K (red circles). (d) Temperature dependence of real part of A.C. susceptibility with different driving frequencies. The low frequency results were shifted upwards for comparison. No spin freezing behaviour was observed down to 50 mK.

effective moment here arises from the combination of crystal electric field and the atomic spin orbit coupling. The Tm^{3+} ion has an electron configuration $4f^{12}$, and atomic spin orbit coupling gives a total angular momentum $J = 6$. The crystal electric field splits the 13-fold degeneracy of the total moment J , and the ground state doublet is a non-Kramers doublet and is regarded as an effective spin-1/2 moment. In principle,

the crystal symmetry of the kagomé lattice forbids any two-fold degeneracy for the integer spin moments and would necessarily create an energy splitting between the two states of the non-Kramers doublet. However, if the energy splitting between these two states is much smaller than the crystal field energy gap that separates these two states from other excited ones, then one can still think the low-temperature magnetic properties of the system are from these non-Kramers doublets. We will discuss this in details in the later part of this article. The negative Θ_{CW} reflects the antiferromagnetic nature of the exchange interactions between the Tm^{3+} local moments in $\text{Tm}_3\text{Sb}_3\text{Zn}_2\text{O}_{14}$. The isothermal magnetization up to 9 T at 2 K and 100 K are shown in Fig. 2(c). At 2 K, the M-H curve starts to deviate from the linear response regime around 2 T, which is consistent with the relatively low energy scale of the interaction between the (low-lying) non-Kramers doublets of the Tm^{3+} ions. In contrast, at 100 K, the excited crystal field states of the Tm^{3+} ions would be thermally excited and contribute to the magnetization. This prevents the magnetization from saturation, and the M-H curve remains linear within our field range. As shown in Fig. 2 (d), A.C. susceptibility of $\text{Tm}_3\text{Sb}_3\text{Zn}_2\text{O}_{14}$ under different driving frequencies was measured down to 50 mK. The Curie-Weiss like behaviour instead of the down turn feature of real part of A.C. susceptibility at low temperatures indicates the absence of spin glass behaviour. Additionally, no signature of transition or separation between zero-field cooling and field cooling procedures (not shown here) was observed, eliminating the possibility of spin glass state.

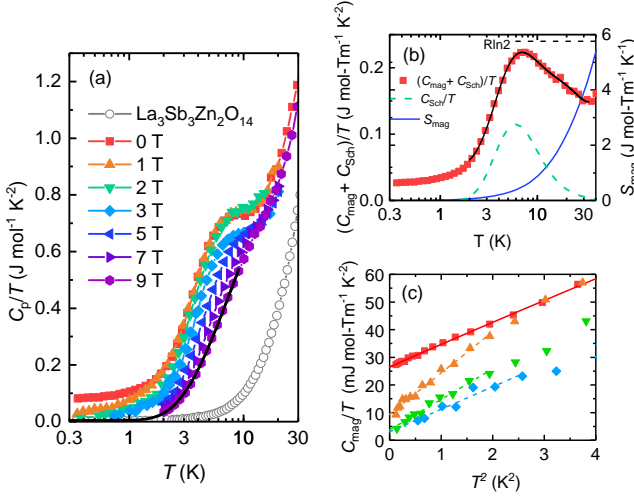


FIG. 3. (a) Specific heat of $\text{Tm}_3\text{Sb}_3\text{Zn}_2\text{O}_{14}$ at different magnetic fields up to 9 T. A Schottky type kink is observed around 9 K at zero field and is gradually suppressed by applying magnetic fields. The solid black line shows the exponential fitting of the 9 T data as described in the main text. The specific heat of non-magnetic $\text{La}_3\text{Sb}_3\text{Zn}_2\text{O}_{14}$ is also shown for comparison. (b) The phonon contribution subtracted specific heat of $\text{Tm}_3\text{Sb}_3\text{Zn}_2\text{O}_{14}$ at zero field. The green dashed curve indicates the fitted Schottky contribution. The blue line is the magnetic entropy change obtained by integrating the magnetic specific heat from the lowest measured temperature. The horizontal dashed line indicates the entropy for spin-1/2 moments $R \ln 2$. (c) Low temperature specific heat coefficient (C_p/T) per mol Tm^{3+} as a function of T^2 . The red line is a linear fit of the zero field data, indicating a finite interception $\gamma(0) = 26.6(1) \text{ mJ mol-Tm}^{-1} \text{K}^{-2}$. $\gamma(0)$ is gradually suppressed by magnetic fields and finally reaches a finite value around 3 T. The dashed lines are guide to the eye.

C. Specific Heat

The magnetic susceptibility and magnetization measurements provide the basic information about the magnetic moments and the interaction energy scale in $\text{Tm}_3\text{Sb}_3\text{Zn}_2\text{O}_{14}$. To reveal the low-energy and low-temperature properties, we measured the specific heat of $\text{Tm}_3\text{Sb}_3\text{Zn}_2\text{O}_{14}$ at different applied magnetic fields. Thanks to the non-magnetic isostructural material $\text{La}_3\text{Sb}_3\text{Zn}_2\text{O}_{14}$, we are able to obtain the phonon contribution to the specific heat. In Fig. 3, we depict the specific heat data of $\text{Tm}_3\text{Sb}_3\text{Zn}_2\text{O}_{14}$ and $\text{La}_3\text{Sb}_3\text{Zn}_2\text{O}_{14}$. At zero magnetic field, a broad hump was observed for $\text{Tm}_3\text{Sb}_3\text{Zn}_2\text{O}_{14}$ around 9 K, which can be fitted by adding a Schottky anomaly term (green dashed curve in Fig. 3(b)), with the gap value $\Delta = 19.4(2) \text{ K}$. The Schottky anomaly should come from the effect of disorder since it was gradually suppressed by the applied magnetic field. No sharp anomaly for magnetic transitions was observed down to the lowest measured temperature

0.35 K, indicating the absence of long range magnetic orders in $\text{Tm}_3\text{Sb}_3\text{Zn}_2\text{O}_{14}$. As is expected, magnetic field does not show any influence on the specific heat of $\text{La}_3\text{Sb}_3\text{Zn}_2\text{O}_{14}$. Moreover, from the comparison in Fig. 3 (a), the phonon contribution to the specific heat of $\text{Tm}_3\text{Sb}_3\text{Zn}_2\text{O}_{14}$ is almost negligible below $\sim 4 \text{ K}$.

The low-temperature specific heat coefficients C_p/T of $\text{Tm}_3\text{Sb}_3\text{Zn}_2\text{O}_{14}$ at different applied magnetic fields are further displayed in Fig. 3 (c). By extrapolating the zero field C_p/T to zero temperature, a finite interception $\gamma(0) = 26.6(1) \text{ mJ mol-Tm}^{-1} \text{K}^{-2}$ is obtained, indicating $C_p \sim \gamma T$ at the low temperature limit. As shown in Fig. 3 (c), by applying magnetic field, the zero temperature specific coefficient $\gamma(0)$ is gradually suppressed. This means that part of $\gamma(0)$ could be induced by the (quenched) disorders^{37,65}. For magnetic field larger than 2 T where the disorder effect can be reduced or removed⁶⁵, $\gamma(0)$ reaches a finite value of $3.7(5) \text{ mJ mol-Tm}^{-1} \text{K}^{-2}$ for 2 T and $3(1) \text{ mJ mol-Tm}^{-1} \text{K}^{-2}$ for 3 T, suggesting there is a constant density of states at low energies and is consistent with a spin liquid state with either spinon Fermi surfaces or a spinon quadratic node at the spinon Fermi energy^{66,67}. Such a linear- T heat capacity was also observed in the organic QSL candidate κ -(BEDT-TTF)₂Cu₂(CN)₃⁸ and $\text{EtMe}_3\text{Sb}[\text{Pd}(\text{dmit})_2]_2$ ⁶⁸. Thus, we propose the candidate spin liquid ground states to be a \mathbb{Z}_2 QSL with either spinon Fermi surfaces or a spinon quadratic touching node at the spinon Fermi energy that give rise to a constant density of states at low energies. A QSL with a continuous gauge group such as $U(1)$ would have a larger density of states than a \mathbb{Z}_2 QSL at low energies due to the soft gauge fluctuations^{66,69}. When even larger magnetic fields are applied, a field-induced gap is obtained. An activated form $C_p \sim e^{-\Delta/T}$ is then used to fit the 9 T data, and we find an energy gap $\Delta = 8.0(1) \text{ K}$ and a tiny residual $\gamma(0) = 1.9(7) \text{ mJ mol-Tm}^{-1} \text{K}^{-2}$. In this high field regime, the Tm^{3+} local moments are polarized to the field direction, the system is in an almost polarized state at low temperatures (see Fig. 2 (c)), and the fitted gap $\Delta = 8.0(1) \text{ K}$ is simply a magnon gap that is induced by external magnetic fields. In Fig. 3 (b), we further subtract the phonon contribution and the Schottky anomaly due to disorder effect and show the calculated magnetic entropy up to 40 K. We find the calculated entropy for zero field reaches $\sim R \ln 2$ that is the entropy for spin-1/2 moments.

D. ZF- μ SR

To further probe the magnetic properties, we implement the ZF- μ SR measurements on $\text{Tm}_3\text{Sb}_3\text{Zn}_2\text{O}_{14}$ down to 20 mK. The ZF- μ SR spectra under two typical temperatures were shown in Fig. 4. No long range order or spin freezing was detected in our sample. This is evidenced by the absence of oscillation behavior (i.e. initial asymmetry loss) in the spectra⁷⁰⁻⁷². The static

random (time-reversal-breaking) field distribution was also excluded due to the lacking of long time recovery to 1/3 of asymmetry, suggesting that the relaxation was caused by dynamic effects⁷³. The ZF- μ SR spectra were further fitted by a single relaxation function:

$$A(t) = A_0 + A_s \left(\frac{1}{3} + \frac{2}{3} e^{-(\lambda t)^\beta} \right), \quad (1)$$

where A_0 is the constant background signal from silver sample holder, λ is the muon spin relaxation rate and β is the stretched exponent. Multiple components in the fitting function, originated from multiple muon stopping sites, do not give better fit quality. In a polycrystal sample, the local-field was randomly oriented and the $\frac{1}{3}$ ($\frac{2}{3}$) term in the fitting function stands for the local-field component parallel (perpendicular) to the initial muon spin. A stretched exponential decay function was usually used to describe the frustrated system^{20,74}. In Fig. 4(b), we show the temperature dependence of relaxation rate λ . As the temperature is decreased, λ gradually increases, saturates below 2 K, and remains almost constant down to the lowest measured temperature 20 mK. The low temperature plateau of λ indicates the persistent spin dynamics and large density of states at low energies⁷⁴. This is consistent with the large density of states from a QSL state with spinon Fermi surface or a spinon quadratic touching node, instead of a gapped state. Moreover, as is shown in Fig. 4 (c), the observed stretched exponent β is found to be ~ 1 and is almost temperature independence, suggesting the absence of obvious disorder/impurity induced relaxation process⁴³. We want to emphasize that previous study shows that for some materials with non-Kramers ions, the measured μ SR response is dominated by an effect resulting from the muon-induced local distortion rather than the intrinsic behavior of the host compound, such as $\text{Pr}_2\text{B}_2\text{O}_7$ ($B = \text{Sn}, \text{Zr}, \text{Hf}$)⁷⁵. However, it does not meet our situation since no such static distribution of magnetic moments observed in $\text{Pr}_2\text{B}_2\text{O}_7$ ⁷⁵ was found in our experiments. Further density functional theory calculations may give more information of the effect of the induced muons. We argue that the dynamic relaxation is caused by the Tm^{3+} ions considering the larger effective magnetic moment. Our result here is quite different from the behaviors in other frustrated antiferromagnets such as spin glass in $\text{Y}_2\text{Mo}_2\text{O}_7$ and $\text{Tb}_2\text{Mo}_2\text{O}_7$ ⁷⁶ that show spin spin freezing, or the magnetic ordered state in $\text{Gd}_2\text{Ti}_2\text{O}_7$ ⁷⁷.

IV. DISCUSSION

Here we explain the microscopic origin and discuss the candidate ground states for $\text{Tm}_3\text{Sb}_3\text{Zn}_2\text{O}_{14}$. Since $\text{Tm}_3\text{Sb}_3\text{Zn}_2\text{O}_{14}$ is a derived compound from the rare-earth pyrochlore material, we start from the rare-earth ions on the pyrochlore lattice. Unlike the organics, $\text{Tm}_3\text{Sb}_3\text{Zn}_2\text{O}_{14}$ is in the strong Mott regime with well-localized $4f$ electrons. For an integer spin moment

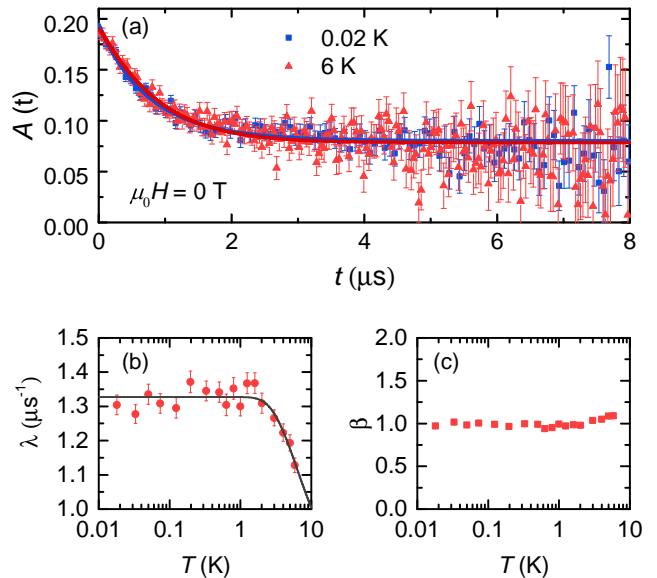


FIG. 4. (a) The ZF- μ SR spectra of $\text{Tm}_3\text{Sb}_3\text{Zn}_2\text{O}_{14}$ measured at different temperatures. Lines are the fitting curves corresponding to the fitting function Eq. (1). The temperature dependence of fitting parameters λ and β are shown in (b) and (c), respectively. The gray curve in (b) is a guide to the eye, indicating the persistent spin dynamics below ~ 2 K.

like the Tm^{3+} ion, the D_{3d} crystal electric field of the pyrochlore lattice can create doubly degenerate ground states that are called non-Kramers doublet, and the transverse (longitudinal) component is the quadrupolar (dipolar) component of the local moment^{78,79}. As we have explained earlier, in a kagomé lattice, the lattice symmetry does not protect the two-fold degeneracy of the non-Kramers doublet any more. The small splitting between two states of the non-Kramers doublet can then be modelled by a *transverse* field that acts on the quadrupolar component of the local spin-1/2 moment^{80,81}. This should be distinguished from the Zeeman coupling to the longitudinal (dipolar) component when the external field is applied to the system^{52,82}. Considering the spin-orbital-entangled nature of the Tm^{3+} non-Kramers doublet, we propose that the magnetic properties of $\text{Tm}_3\text{Sb}_3\text{Zn}_2\text{O}_{14}$ should be governed by the anisotropic spin exchange interaction⁷⁸ and the transverse Zeeman couplings⁸⁰ on the kagomé lattice. Thus the physics here is fundamentally different from the Cu-based herbertsmithite material that is a well-known kagomé lattice spin liquid candidate^{34–36,83}. The theoretical problem for future work is whether the proposed model can give rise to the observed phenomena.

The possible QSL ground state, that we propose for $\text{Tm}_3\text{Sb}_3\text{Zn}_2\text{O}_{14}$, is a \mathbb{Z}_2 QSL with either spinon Fermi surfaces or a spinon quadratic band touching node at the Fermi level. Our thermodynamic measurements cannot distinguish these two QSL states. The inelastic neutron

scattering measurement, however, should observe different results for these two QSL states even with polycrystal samples. For spinon Fermi surfaces, the low energy scattering would extend a finite range of momenta in the reciprocal space^{19,23}. In contrast, the spinon quadratic band touching would produce the spinon continuum near the Brillouin zone center at low energies. This distinction does not require the angular information of the momenta.

Finally, we comment on the non-QSL possibility caused by the disorder effect in $\text{Tm}_3\text{Sb}_3\text{Zn}_2\text{O}_{14}$. Disorder effects are found in this material from XRD refinement. Tm/Zn site disorder in kagomé lattice may modify the spin-spin correlations, and tune the low temperature ground state. The disorder effect in the Cu-based kagomé structure materials is still under debate^{84,85}. Recent theoretical works show that disorder effect could lead to mimicry of spin liquid like behavior in YbMgGaO_4 ⁸⁶. Unlike the Yb^{3+} Kramers doublet in YbMgGaO_4 whose degeneracy is protected by time reversal symmetry^{17–19,21}, the non-Kramers doublet is more susceptible to crystalline disorder. If there exists a crystal field randomness for the Tm^{3+} ion, it would lead to a distribution of the transverse fields on the quadrupolar component of the Tm^{3+} non-Kramers doublet, and the system can then be thought as a localized two-level system with a random distribution of barrier heights and asymmetry energies and could give a constant density of low-energy states^{87,88}. It is interesting both theoretically and experimentally how to distinguish this scenario from the QSL proposal. Recently, Kimchi *et al.* analyzed the effect of quenched disorder on frustrated quantum magnets, and gave a phenomenological description of the observed power-law magnetic specific heat with an anomalous exponent⁶¹. In their random-singlet-inspired picture, the anomalous $C(T)$ exponent is an effective exponent over a range of temperature scales, and can take different values

depending on the disorder distribution⁶¹. Therefore, we can not rule out that the exotic properties are induced by the Tm/Zn site-mixing disorder in $\text{Tm}_3\text{Sb}_3\text{Zn}_2\text{O}_{14}$. On the other hand, we also noticed that disorder can induce QSL state in spin ice pyrochlores⁸⁰.

V. CONCLUSION

To summarize, we have studied the crystal structure, magnetic properties, specific heat and μSR spectra of $\text{Tm}_3\text{Sb}_3\text{Zn}_2\text{O}_{14}$. No long range magnetic order was observed down to 20 mK. Spin freezing behavior was precluded by A.C. susceptibility measurements. A linear- T dependence of low temperature magnetic specific heat was observed, indicating a constant density of low-energy states. The ZF- μSR results suggest persistent spin dynamics at low temperature range. We propose possible QSL ground states and provide the microscopic origin for the magnetic properties of $\text{Tm}_3\text{Sb}_3\text{Zn}_2\text{O}_{14}$.

Acknowledgments.—We wish to thank B. Hitti, and D. Arsenau of the TRIUMF CMMS group for the assistance during the experiments. We also acknowledge Martin Mourigal for an email correspondence, Yi Zhou from Zhejiang University for a discussion, Patrick Lee for a recent comment about the specific heat. We thank Zhong Wang from IAS Tsinghua Univeristy for hospitality where this paper is completed. This work is supported by the National Key Research and Development Program of China (Nos.2016YFA0300503 (L.S.), 2016YFA0301001 (G.C.)), the start-up fund and the first-class university construction fund of Fudan University (G.C.), the thousand-youth-talent program of China (G.C.), and the National Natural Science Foundation of China No.11474060 (L.S.) and No.11774061 (L.S.).

* gangchen.physics@gmail.com

† leishu@fudan.edu.cn

¹ P. W. Anderson, “The Resonating Valence Bond State in La_2CuO_4 and Superconductivity,” *Science* **235**, 1196–1198 (1987).

² P. A. Lee, “An End to the Drought of Quantum Spin Liquids,” *Science* **321**, 1306–1307 (2008).

³ L. Balents, “Spin liquids in frustrated magnets,” *Nature* **464**, 199–208 (2010).

⁴ Y. Zhou, K. Kanoda, and T. Ng, “Quantum spin liquid states,” *Rev. Mod. Phys.* **89**, 025003 (2017).

⁵ Y. Shimizu, K. Miyagawa, K. Kanoda, M. Maesato, and G. Saito, “Spin Liquid State in an Organic Mott Insulator with a Triangular Lattice,” *Phys. Rev. Lett.* **91**, 107001 (2003).

⁶ Y. Shimizu, K. Miyagawa, K. Kanoda, M. Maesato, and G. Saito, “Emergence of inhomogeneous moments from spin liquid in the triangular-lattice Mott insulator $\kappa\text{-(ET)}_2\text{Cu}_2(\text{CN})_3$,” *Phys. Rev. B* **73**, 140407 (2006).

⁷ S. Ohira, Y. Shimizu, K. Kanoda, and G. Saito, “Spin Liquid State in $\kappa\text{-(BEDT-TTF)}_2\text{Cu}_2(\text{CN})_3$ Studied by Muon Spin Relaxation Method,” *J. Low Temp. Phys.* **142**, 153–158 (2007).

⁸ S. Yamashita, Y. Nakazawa, M. Oguni, Y. Oshima, H. Nojiri, Y. Shimizu, K. Miyagawa, and K. Kanoda, “Thermodynamic properties of a spin-1/2 spin-liquid state in a κ -type organic salt,” *Nat. Phys.* **4**, 459–462 (2008).

⁹ F. L. Pratt, P. J. Baker, S. J. Blundell, T. Lancaster, S. Ohira-Kawamura, C. Baines, Y. Shimizu, K. Kanoda, I. Watanabe, and G. Saito, “Magnetic and non-magnetic phases of a quantum spin liquid,” *Nature* **471**, 612–616 (2011).

¹⁰ S. Nakajima, T. Suzuki, Y. Ishii, K. Ohishi, I. Watanabe, T. Goto, A. Oosawa, N. Yoneyama, N. Kobayashi, F. L. Pratt, and T. Sasaki, “Microscopic Phase Separation in Triangular-Lattice Quantum Spin Magnet $\kappa\text{-(BEDT-TTF)}_2\text{Cu}_2(\text{CN})_3$ Probed by Muon Spin Relaxation,” *J. Phys. Soc. Jpn.* **81**, 063706 (2012).

- ¹¹ T. Isono, T. Terashima, K. Miyagawa, K. Kanoda, and S. Uji, “Quantum criticality in an organic spin-liquid insulator κ -(BEDT-TTF)₂Cu₂(CN)₃,” *Nat. Commun.* **7**, 13494 (2016).
- ¹² T. Itou, A. Oyamada, S. Maegawa, M. Tamura, and R. Kato, “Spin-liquid state in an organic spin-1/2 system on a triangular lattice, EtMe₃Sb[Pd(dmit)₂]₂,” *J. Phys.: Condens. Matter* **19**, 145247 (2007).
- ¹³ T. Itou, A. Oyamada, S. Maegawa, M. Tamura, and R. Kato, “Quantum spin liquid in the spin-1/2 triangular antiferromagnet EtMe₃Sb[Pd(dmit)₂]₂,” *Phys. Rev. B* **77**, 104413 (2008).
- ¹⁴ T. Itou, A. Oyamada, S. Maegawa, and R. Kato, “Instability of a quantum spin liquid in an organic triangular-lattice antiferromagnet,” *Nat. Phys.* **6**, 673–676 (2010).
- ¹⁵ Shaginyan, V. R., Msezane, A. Z., Popov, K. G., Japaridze, G. S., and Khodel, V. A., “Heat transport in magnetic fields by quantum spin liquid in the organic insulators EtMe₃Sb[Pd(dmit)₂]₂ and κ -(BEDT-TTF)₂Cu₂(CN)₃,” *Europhys. Lett.* **103**, 67006 (2013).
- ¹⁶ Y. Li, H. Liao, Z. Zhang, S. Li, F. Jin, L. Ling, L. Zhang, Y. Zou, L. Pi, Z. Yang, J. Wang, Z. Wu, and Q. Zhang, “Gapless quantum spin liquid ground state in the two-dimensional spin-1/2 triangular antiferromagnet YbMgGaO₄,” *Sci. Rep.* **5**, 16419 (2015).
- ¹⁷ Y. Li, G. Chen, W. Tong, L. Pi, J. Liu, Z. Yang, X. Wang, and Q. Zhang, “Rare-Earth Triangular Lattice Spin Liquid: A Single-Crystal Study of YbMgGaO₄,” *Phys. Rev. Lett.* **115**, 167203 (2015).
- ¹⁸ Y.-D. Li, X. Wang, and G. Chen, “Anisotropic spin model of strong spin-orbit-coupled triangular antiferromagnets,” *Phys. Rev. B* **94**, 035107 (2016).
- ¹⁹ Y. Shen, Y.-D. Li, H. Wo, Y. Li, S. Shen, B. Pan, Q. Wang, H. C. Walker, P. Steffens, M. Boehm, Y. Hao, D. L. Quintero-Castro, L. W. Harriger, M. D. Frontzek, L. Hao, S. Meng, Q. Zhang, G. Chen, and J. Zhao, “Evidence for a spinon Fermi surface in a triangular-lattice quantum-spin-liquid candidate,” *Nature* **540**, 559–562 (2016).
- ²⁰ Y. Li, D. Adroja, P. K. Biswas, P. J. Baker, Q. Zhang, J. Liu, A. A. Tsirlin, P. Gegenwart, and Q. Zhang, “Muon Spin Relaxation Evidence for the U(1) Quantum Spin-Liquid Ground State in the Triangular Antiferromagnet YbMgGaO₄,” *Phys. Rev. Lett.* **117**, 097201 (2016).
- ²¹ J. A. M. Paddison, Z. Dun, G. Ehlers, Y. Liu, M. B. Stone, H. g Zhou, and M. Mourigal, “Continuous excitations of the triangular-lattice quantum spin liquid YbMgGaO₄,” *Nat. Phys.* **13**, 117–122 (2017).
- ²² Y. Xu, J. Zhang, Y. S. Li, Y. J. Yu, X. C. Hong, Q. M. Zhang, and S. Y. Li, “Absence of Magnetic Thermal Conductivity in the Quantum Spin-Liquid Candidate YbMgGaO₄,” *Phys. Rev. Lett.* **117**, 267202 (2016).
- ²³ Y.-D. Li, Y.-M. Lu, and G. Chen, “Spinon Fermi surface U(1) spin liquid in the spin-orbit-coupled triangular-lattice Mott insulator YbMgGaO₄,” *Phys. Rev. B* **96**, 054445 (2017).
- ²⁴ C. Liu, R. Yu, and X. Wang, “Semiclassical ground-state phase diagram and multi-*Q* phase of a spin-orbit-coupled model on triangular lattice,” *Phys. Rev. B* **94**, 174424 (2016).
- ²⁵ Z. Zhu, P. A. Maksimov, S. R. White, and A. L. Chernyshev, “Disorder-Induced Mimicry of a Spin Liquid in YbMgGaO₄,” *Phys. Rev. Lett.* **119**, 157201 (2017).
- ²⁶ Z.-X. Luo, E. Lake, J.-W. Mei, and O. A. Starykh, “Spinon Magnetic Resonance of Quantum Spin Liquids,” *Phys. Rev. Lett.* **120**, 037204 (2018).
- ²⁷ Y.-D. Li and G. Chen, “Detecting spin fractionalization in a spinon Fermi surface spin liquid,” *Phys. Rev. B* **96**, 075105 (2017).
- ²⁸ Y.-D. Li, Y. Shen, Y. Li, J. Zhao, and G. Chen, “Effect of spin-orbit coupling on the effective-spin correlation in ybmga₄,” *Phys. Rev. B* **97**, 125105 (2018).
- ²⁹ Y. Li, D. Adroja, R. I. Bewley, D. Voneshen, A. A. Tsirlin, P. Gegenwart, and Q. Zhang, “Crystalline Electric-Field Randomness in the Triangular Lattice Spin-Liquid YbMgGaO₄,” *Phys. Rev. Lett.* **118**, 107202 (2017).
- ³⁰ S. Toth, K. Rolfs, A. R. Wildes, and C. Ruegg, “Strong exchange anisotropy in YbMgGaO₄ from polarized neutron diffraction,” *arXiv preprint arXiv:1705.05699* (2017).
- ³¹ Y. Shen, Y.-D. Li, H. C. Walker, P. Steffens, M. Boehm, X. Zhang, S. Shen, H. g Wo, G. Chen, and J. Zhao, “Fractionalized excitations in the partially magnetized spin liquid candidate YbMgGaO₄,” *arXiv preprint arXiv:1708.06655* (2017).
- ³² X. Zhang, F. Mahmood, M. Daum, Z. Dun, J. A. M. Paddison, N. J. Laurita, T. Hong, H. Zhou, N. P. Armitage, and M. Mourigal, “Hierarchy of exchange interactions in the triangular-lattice spin-liquid YbMgGaO₄,” *arXiv preprint 1708.07503* (2017).
- ³³ Z. Ma, J. Wang, Z.-Y. Dong, J. Zhang, S. Li, S.-H. Zheng, Y. Yu, W. Wang, L. Che, K. Ran, S. Bao, Z. Cai, P. Čermák, A. Schneidewind, S. Yano, J. S. Gardner, X. Lu, S.-L. Yu, J.-M. Liu, S. Li, J.-X. Li, and J. Wen, “Spin-Glass Ground State in a Triangular-Lattice Compound YbZnGaO₄,” *Phys. Rev. Lett.* **120**, 087201 (2018).
- ³⁴ J. S. Helton, K. Matan, M. P. Shores, E. A. Nytko, B. M. Bartlett, Y. Yoshida, Y. Takano, A. Suslov, Y. Qiu, J.-H. Chung, D. G. Nocera, and Y. S. Lee, “Spin Dynamics of the Spin-1/2 Kagome Lattice Antiferromagnet ZnCu₃(OH)₆Cl₂,” *Phys. Rev. Lett.* **98**, 107204 (2007).
- ³⁵ T.-H. Han, J. S. Helton, S. Chu, D. G. Nocera, J. A. Rodriguez-Rivera, C. Broholm, and Y. S. Lee, “Fractionalized excitations in the spin-liquid state of a kagome-lattice antiferromagnet,” *Nature* **492**, 406 (2012).
- ³⁶ M. Fu, T. Imai, T.-H. Han, and Y. S. Lee, “Evidence for a gapped spin-liquid ground state in a kagome Heisenberg antiferromagnet,” *Science* **350**, 655–658 (2015).
- ³⁷ Y. Okamoto, M. Nohara, H. Aruga-Katori, and H. Takagi, “Spin-Liquid State in the *S* = 1/2 Hyperkagome Antiferromagnet Na₄Ir₃O₈,” *Phys. Rev. Lett.* **99**, 137207 (2007).
- ³⁸ G. Chen and L. Balents, “Spin-orbit effects in Na₄Ir₃O₈: A hyper-kagome lattice antiferromagnet,” *Phys. Rev. B* **78**, 094403 (2008).
- ³⁹ Y. Zhou, P. A. Lee, T.-K. Ng, and F.-C. Zhang, “Na₄Ir₃O₈ as a 3D Spin Liquid with Fermionic Spinons,” *Phys. Rev. Lett.* **101**, 197201 (2008).
- ⁴⁰ D. Pröpper, A. N. Yaresko, T. I. Larkin, T. N. Stanislavchuk, A. A. Sirenko, T. Takayama, A. Matsumoto, H. Takagi, B. Keimer, and A. V. Boris, “Fano Resonances in the Infrared Spectra of Phonons in Hyperkagome Na₃Ir₃O₈,” *Phys. Rev. Lett.* **112**, 087401 (2014).
- ⁴¹ G. Chen and Y. B. Kim, “Anomalous enhancement of the Wilson ratio in a quantum spin liquid: The case of Na₄Ir₃O₈,” *Phys. Rev. B* **87**, 165120 (2013).

- ⁴² R. Dally, T. Hogan, A. Amato, H. Luetkens, C. Baines, J. Rodriguez-Rivera, M. J. Graf, and S. D. Wilson, “Short-Range Correlations in the Magnetic Ground State of $\text{Na}_4\text{Ir}_3\text{O}_8$,” *Phys. Rev. Lett.* **113**, 247601 (2014).
- ⁴³ A. Yaouanc, P. Dalmas de Réotier, C. Marin, and V. Glazkov, “Single-crystal versus polycrystalline samples of magnetically frustrated $\text{Yb}_2\text{Ti}_2\text{O}_7$: Specific heat results,” *Phys. Rev. B* **84**, 172408 (2011).
- ⁴⁴ K. A. Ross, L. Savary, B. D. Gaulin, and L. Balents, “Quantum excitations in quantum spin ice,” *Phys. Rev. X* **1**, 021002 (2011).
- ⁴⁵ K. Matsuhira, C. Sekine, C. Paulsen, M. Wakeshima, Y. Hinatsu, T. Kitazawa, Y. Kiuchi, Z. Hiroi, and S. Takagi, “Spin freezing in the pyrochlore antiferromagnet $\text{Pr}_2\text{Zr}_2\text{O}_7$,” *J. Phys.: Conf. Ser.* **145**, 012031 (2009).
- ⁴⁶ S. Nakatsuji, Y. Machida, Y. Maeno, T. Tayama, T. Sakakibara, J. van Duijn, L. Balicas, J. N. Millican, R. T. Macaluso, and Julia Y. Chan, “Metallic Spin-Liquid Behavior of the Geometrically Frustrated Kondo Lattice $\text{Pr}_2\text{Ir}_2\text{O}_7$,” *Phys. Rev. Lett.* **96**, 087204 (2006).
- ⁴⁷ Y. Machida, S. Nakatsuji, S. Onoda, T. Tayama, and T. Sakakibara, “Time-reversal symmetry breaking and spontaneous Hall effect without magnetic dipole order,” *Nature* **463**, 210–213 (2009).
- ⁴⁸ Y. Tokiwa, J. J. Ishikawa, S. Nakatsuji, and P. Gegenwart, “Quantum criticality in a metallic spin liquid,” *Nat. Mater.* **13**, 356 (2014).
- ⁴⁹ D. E. MacLaughlin, O. O. Bernal, L. Shu, J. Ishikawa, Y. Matsumoto, J.-J. Wen, M. Mourigal, C. Stock, G. Ehlers, C. L. Broholm, Y. Machida, K. Kimura, S. Nakatsuji, Y. Shimura, and T. Sakakibara, “Unstable spin-ice order in the stuffed metallic pyrochlore $\text{Pr}_{2+x}\text{Ir}_{2-x}\text{O}_{7-\delta}$,” *Phys. Rev. B* **92**, 054432 (2015).
- ⁵⁰ G. Chen, ““Magnetic monopole” condensation of the pyrochlore ice $\text{U}(1)$ quantum spin liquid: Application to $\text{Pr}_2\text{Ir}_2\text{O}_7$ and $\text{Yb}_2\text{Ti}_2\text{O}_7$,” *Phys. Rev. B* **94**, 205107 (2016).
- ⁵¹ B. Cheng, T. Ohtsuki, D. Chaudhuri, S. Nakatsuji, M. Lippmaa, and N. P. Armitage, “Dielectric anomalies and interactions in the three-dimensional quadratic band touching Luttinger semimetal $\text{Pr}_2\text{Ir}_2\text{O}_7$,” *Nat. Commun.* **8**, 2097 (2017).
- ⁵² X.-P. Yao and G. Chen, “ $\text{Pr}_2\text{Ir}_2\text{O}_7$: when Luttinger semimetal meets Melko-Hertog-Gingras spin ice state,” *arXiv preprint 1712.06534* (2017).
- ⁵³ M. J. P. Gingras, B. C. den Hertog, M. Faucher, J. S. Gardner, S. R. Dunsiger, L. J. Chang, B. D. Gaulin, N. P. Raju, and J. E. Greedan, “Thermodynamic and single-ion properties of Tb^{3+} within the collective paramagnetic-spin liquid state of the frustrated pyrochlore antiferromagnet $\text{Tb}_2\text{Ti}_2\text{O}_7$,” *Phys. Rev. B* **62**, 6496–6511 (2000).
- ⁵⁴ H. Takatsu, H. Kadowaki, T. J. Sato, J. W. Lynn, Y. Tabata, T. Yamazaki, and K. Matsuhira, “Quantum spin fluctuations in the spin-liquid state of $\text{Tb}_2\text{Ti}_2\text{O}_7$,” *J. Phys.: Condens. Matter* **24**, 052201 (2012).
- ⁵⁵ M. B. Sanders, J. W. Krizan, and R. J. Cava, “ $\text{RE}_3\text{Sb}_3\text{Zn}_2\text{O}_{14}$ ($\text{RE} = \text{La}, \text{Pr}, \text{Nd}, \text{Sm}, \text{Eu}, \text{Gd}$): a new family of pyrochlore derivatives with rare earth ions on a 2D Kagome lattice,” *J. Mater. Chem. C* **4**, 541–550 (2016).
- ⁵⁶ Z. L. Dun, J. Trinh, K. Li, M. Lee, K. W. Chen, R. Baumbach, Y. F. Hu, Y. X. Wang, E. S. Choi, B. S. Shastry, A. P. Ramirez, and H. D. Zhou, “Magnetic Ground States of the Rare-Earth Tripod Kagome Lattice $\text{Mg}_2\text{RE}_3\text{Sb}_3\text{O}_{14}$ ($\text{RE} = \text{Gd}, \text{Dy}, \text{Er}$),” *Phys. Rev. Lett.* **116**, 157201 (2016).
- ⁵⁷ A. Scheie, M. Sanders, J. Krizan, Y. Qiu, R. J. Cava, and C. Broholm, “Effective spin-1/2 scalar chiral order on kagome lattices in $\text{Nd}_3\text{Sb}_3\text{Mg}_2\text{O}_{14}$,” *Phys. Rev. B* **93**, 180407 (2016).
- ⁵⁸ J. A. M. Paddison, H. S. Ong, J. O. Hamp, P. Mukherjee, X. Bai, M. G. Tucker, N. P. Butch, C. Castelnovo, M. Mourigal, and S. E. Dutton, “Emergent order in the kagome Ising magnet $\text{Dy}_3\text{Mg}_2\text{Sb}_3\text{O}_{14}$,” *Nat. Commun.* **7**, 13842 (2016).
- ⁵⁹ Z. L. Dun, J. Trinh, M. Lee, E. S. Choi, K. Li, Y. F. Hu, Y. X. Wang, N. Blanc, A. P. Ramirez, and H. D. Zhou, “Structural and magnetic properties of two branches of the tripod-kagome-lattice family $\text{A}_2\text{R}_3\text{Sb}_3\text{O}_{14}$ ($\text{A} = \text{Mg}, \text{Zn}$; $\text{R} = \text{Pr}, \text{Nd}, \text{Gd}, \text{Tb}, \text{Dy}, \text{Ho}, \text{Er}, \text{Yb}$),” *Phys. Rev. B* **95**, 104439 (2017).
- ⁶⁰ Z. L. Dun, X. J. Bai, J. A. M. Paddison, N. P. Butch, C. D. Cruz, M. B. Stone, T. Hong, M. Mourigal, and H. D. Zhou, “Quantum Spin Fragmentation in Kagome Ice $\text{Ho}_3\text{Mg}_2\text{Sb}_3\text{O}_{14}$,” *arXiv preprint arXiv:1806.04081* (2018).
- ⁶¹ I. Kimchi, A. Nahum, and T. Senthil, “Valence bonds in random quantum magnets: Theory and application to ybmgao_4 ,” *Phys. Rev. X* **8**, 031028 (2018).
- ⁶² B. H. Toby and R. B. V. Dreele, “*GSAS-II*: the genesis of a modern open-source all purpose crystallography software package,” *J. Appl. Crystallogr.* **46**, 544–549 (2013).
- ⁶³ B. H. Toby, “*EXPGUI*, a graphical user interface for *gsas*,” *J. Appl. Crystallogr.* **34**, 210–213 (2001).
- ⁶⁴ G. D. Morris and R. H. Heffner, “A method of achieving accurate zero-field conditions using muonium,” *Physica B: Condensed Matter* **326**, 252 – 254 (2003).
- ⁶⁵ I. Kimchi, J. P. Shekelton, T. M. McQueen, and P. A. Lee, “Heat capacity from local moments in frustrated disordered quantum spin systems: scaling and data collapse,” *arXiv preprint 1803.00013* (2018).
- ⁶⁶ S.-S. Lee and P. A. Lee, “ $\text{U}(1)$ Gauge Theory of the Hubbard Model: Spin Liquid States and Possible Application to κ -(BEDT-TTF) $_2\text{Cu}_2(\text{CN})_3$,” *Phys. Rev. Lett.* **95**, 036403 (2005).
- ⁶⁷ R. V. Mishmash, J. R. Garrison, S. Bieri, and C. Xu, “Theory of a Competitive Spin Liquid State for Weak Mott Insulators on the Triangular Lattice,” *Phys. Rev. Lett.* **111**, 157203 (2013).
- ⁶⁸ S. Yamashita, T. Yamamoto, Y. Nakazawa, M. Tamura, and R. Kato, “Gapless spin liquid of an organic triangular compound evidenced by thermodynamic measurements,” *Nat. Commun.* **2**, 275 (2011).
- ⁶⁹ P. A. Lee and N. Nagaosa, “Gauge theory of the normal state of high- T_c superconductors,” *Phys. Rev. B* **46**, 5621–5639 (1992).
- ⁷⁰ A. Keren, K. Kojima, L. P. Le, G. M. Luke, W. D. Wu, Y. J. Uemura, M. Takano, H. Dabkowska, and M. J. P. Gingras, “Muon-spin-rotation measurements in the kagomé lattice systems: Cr-jarosite and Fe-jarosite,” *Phys. Rev. B* **53**, 6451–6454 (1996).
- ⁷¹ X. G. Zheng, H. Kubozono, K. Nishiyama, W. Higemoto, T. Kawae, A. Koda, and C. N. Xu, “Coexistence of Long-Range Order and Spin Fluctuation in Geometrically Frustrated Clinoatacamite $\text{Cu}_2\text{Cl}(\text{OH})_3$,” *Phys. Rev. Lett.* **95**, 057201 (2005).
- ⁷² X. F. Miao, L. Caron, J. Cedervall, P. C. M. Gubbens, P. Dalmas de Réotier, A. Yaouanc, F. Qian, A. R. Wildes, H. Luetkens, A. Amato, N. H. van Dijk, and E. Brück, “Short-range magnetic correlations and spin dynamics in the paramagnetic regime of $(\text{Mn}, \text{Fe})_2(\text{P}, \text{Si})$,” *Phys. Rev.*

- [B 94, 014426 \(2016\)](#).
- ⁷³ Y. J. Uemura, T. Yamazaki, D. R. Harshman, M. Senba, and E. J. Ansaldo, “Muon-spin relaxation in AuFe and CuMn spin glasses,” *Phys. Rev. B* **31**, 546–563 (1985).
- ⁷⁴ Y. J. Uemura, A. Keren, K. Kojima, L. P. Le, G. M. Luke, W. D. Wu, Y. Ajiro, T. Asano, Y. Kuriyama, M. Mekata, H. Kikuchi, and K. Kakurai, “Spin fluctuations in frustrated kagome lattice system $\text{SrCr}_8\text{Ga}_4\text{O}_{19}$ studied by muon spin relaxation,” *Phys. Rev. Lett.* **73**, 3306–3309 (1994).
- ⁷⁵ F. R. Foronda, F. Lang, J. S. Moller, T. Lancaster, A. T. Boothroyd, F. L. Pratt, S. R. Giblin, D. Prabhakaran, and S. J. Blundell, “Anisotropic local modification of crystal field levels in pr-based pyrochlores: a muon-induced effect modeled using density functional theory,” *Phys. Rev. Lett.* **114**, 017602 (2015).
- ⁷⁶ S. R. Dunsiger, R. F. Kiefl, K. H. Chow, B. D. Gaulin, M. J. P. Gingras, J. E. Greedan, A. Keren, K. Kojima, G. M. Luke, W. A. MacFarlane, N. P. Raju, J. E. Sonier, Y. J. Uemura, and W. D. Wu, “Muon spin relaxation investigation of the spin dynamics of geometrically frustrated antiferromagnets $\text{Y}_2\text{Mo}_2\text{O}_7$ and $\text{Tb}_2\text{Mo}_2\text{O}_7$,” *Phys. Rev. B* **54**, 9019–9022 (1996).
- ⁷⁷ S. R. Dunsiger, R. F. Kiefl, J. A. Chakhalian, J. E. Greedan, W. A. MacFarlane, R. I. Miller, G. D. Morris, A. N. Price, N. P. Raju, and J. E. Sonier, “Magnetic field dependence of muon spin relaxation in geometrically frustrated $\text{Gd}_2\text{Ti}_2\text{O}_7$,” *Phys. Rev. B* **73**, 172418 (2006).
- ⁷⁸ S. H. Curnoe, “Structural distortion and the spin liquid state in $\text{Tb}_2\text{Ti}_2\text{O}_7$,” *Phys. Rev. B* **78**, 094418 (2008).
- ⁷⁹ S. Onoda and Y. Tanaka, “Quantum Melting of Spin Ice: Emergent Cooperative Quadrupole and Chirality,” *Phys. Rev. Lett.* **105**, 047201 (2010).
- ⁸⁰ L. Savary and L. Balents, “Disorder-induced quantum spin liquid in spin ice pyrochlores,” *Phys. Rev. Lett.* **118**, 087203 (2017).
- ⁸¹ J.-J. Wen, S. M. Koohpayeh, K. A. Ross, B. A. Trump, T. M. McQueen, K. Kimura, S. Nakatsuji, Y. Qiu, D. M. Pajerowski, J. R. D. Copley, and C. L. Broholm, “Disordered Route to the Coulomb Quantum Spin Liquid: Random Transverse Fields on Spin Ice in $\text{Pr}_2\text{Zr}_2\text{O}_7$,” *Phys. Rev. Lett.* **118**, 107206 (2017).
- ⁸² G. Chen, “Dirac’s “magnetic monopoles” in pyrochlore ice $U(1)$ spin liquids: Spectrum and classification,” *Phys. Rev. B* **96**, 195127 (2017).
- ⁸³ Y. Ran, M. Hermele, P. A. Lee, and X.-G. Wen, “Projected-Wave-Function Study of the Spin-1/2 Heisenberg Model on the Kagomé Lattice,” *Phys. Rev. Lett.* **98**, 117205 (2007).
- ⁸⁴ T.-H. Han, M. R. Norman, J. J. Wen, J. A. Rodriguez-Rivera, J. S. Helton, C. Broholm, and Y. S. Lee, “Correlated impurities and intrinsic spin-liquid physics in the kagome material herbertsmithite,” *Phys. Rev. B* **94**, 060409 (2016).
- ⁸⁵ Z. Feng, Z. Li, X. Meng, W. Yi, Y. Wei, J. Zhang, Y.-C. Wang, W. Jiang, Z. Liu, S. Li, F. Liu, J. Luo, S. Li, G.-Q. Zheng, Z. Y. Meng, J.-W. Mei, and Y. Shi, “Gapped Spin-1/2 Spinon Excitations in a New Kagome Quantum Spin Liquid Compound $\text{Cu}_3\text{Zn}(\text{OH})_6\text{FBr}$,” *Chin. Phys. Lett.* **34**, 077502 (2017).
- ⁸⁶ Z. Zhu, P. A. Maksimov, S. R. White, and A. L. Chernyshev, “Disorder-Induced Mimicry of a Spin Liquid in YbMgGaO_4 ,” *Phys. Rev. Lett.* **119**, 157201 (2017).
- ⁸⁷ P. W. Anderson, B. I. Halperin, and C. M. Varma, “Anomalous low-temperature thermal properties of glasses and spin glasses,” *Phil. Mag.* **25**, 1–9 (1972).
- ⁸⁸ M. P. Solf and M. W. Klein, “Two-level tunneling states and the constant density of states in quadrupolar glasses,” *Phys. Rev. B* **49**, 12703–12717 (1994).